





# Effect of Local Thermal Equilibrium Misbalance on Long-wavelength Slow Magnetoacoustic Waves

V. M. Nakariakov<sup>1,2</sup> , A. N. Afanasyev<sup>3</sup>, S. Kumar<sup>2</sup>, and Y.-J. Moon<sup>2</sup> 

<sup>1</sup> Centre for Fusion, Space and Astrophysics, Physics Department, University of Warwick, Coventry CV4 7AL, UK; [V.Nakariakov@warwick.ac.uk](mailto:V.Nakariakov@warwick.ac.uk)

<sup>2</sup> School of Space Research, Kyung Hee University, Yongin, 446-701, Gyeonggi, Korea

<sup>3</sup> Institute of Solar-Terrestrial Physics SB RAS, P.O. Box 291, Lermontov St. 126A, Irkutsk 664033, Russia

Received 2017 September 13; accepted 2017 September 18; published 2017 October 31

## Abstract

Evolution of slow magnetoacoustic waves guided by a cylindrical magnetic flux tube that represents a coronal loop or plume, is modeled accounting for the effects of finite gas pressure, weak nonlinearity, dissipation by thermal conduction and viscosity, and the misbalance between the cooling by optically thin radiation and unspecified heating of the plasma. An evolutionary equation of the Burgers–Malthus type is derived. It is shown that the cooling/heating misbalance, determined by the derivatives of the combined radiative cooling and heating function, with respect to the density, temperature, and magnetic field at the thermal equilibrium affect the wave rather strongly. This effect may either cause additional damping, or counteract it, or lead to the gradual amplification of the wave. In the latter case, the coronal plasma acts as an active medium for the slow magnetoacoustic waves. The effect of the cooling/heating misbalance could be important for coronal slow waves, and could be responsible for certain discrepancies between theoretical results and observations, in particular, the increased or decreased damping lengths and times, detection of the waves at certain heights only, and excitation of compressive oscillations. The results obtained open up a possibility for the diagnostics of the coronal heating function by slow magnetoacoustic waves.

*Key words:* magnetohydrodynamics (MHD) – Sun: corona – Sun: oscillations – waves

## 1. Introduction

Magnetohydrodynamic (MHD) waves are detected everywhere in the solar atmosphere, and play a significant role in the structure and dynamics of the corona (see, e.g., Jess et al. 2015; Nakariakov et al. 2016, for recent comprehensive reviews). During the last few decades, these waves have been intensively studied observationally, from ground- and space-based instruments, and theoretically, in particular, as a possible source of coronal plasma heating and solar wind acceleration. In addition, the waves provide us with important seismological information about the physical parameters of the corona, which are difficult or even impossible to measure directly. The seismological diagnostics not only provide the information about the physical parameters of the medium, but also allows us to reveal main physical mechanisms operating in the plasma. In particular, seismological techniques could be used for the evaluation of the relative importance of different heating mechanisms (e.g., De Moortel & Browning 2015) and the determination of the coronal heating function.

Coronal oscillations are often observed as propagating quasi-periodic extreme-ultraviolet (EUV) and soft X-ray intensity disturbances, in particular, with the high-resolution imaging telescopes *SOHO*/EIT (e.g., DeForest & Gurman 1998; Berghmans & Clette 1999), *TRACE* (e.g., De Moortel et al. 2000; De Moortel 2009), *SDO*/AIA (e.g., Kiddie et al. 2012; Krishna Prasad et al. 2012; Su 2014), and *Hinode*/XRT (e.g., Sakao et al. 2007). These propagating quasi-periodic disturbances are usually detected in legs of long loops and in open coronal structures, for example, in polar plumes. These waves are essentially compressive, and propagate along the apparent direction of the magnetic field, at approximately the local sound speed that is determined by the plasma temperature (e.g., Marsh et al. 2009; Yuan & Nakariakov 2012),

and are therefore confidently interpreted as propagating slow magnetoacoustic waves. Propagating compressive waves detected in coronal loops and in polar plumes appear to be similar, with the exception that the oscillation period in plumes is typically longer than in loops (e.g., Nakariakov 2006; Krishna Prasad et al. 2014). However, long period oscillations have been detected in loops of plasma fans of coronal active regions too (e.g., Yuan et al. 2011; Krishna Prasad et al. 2012; Abedini 2016). These waves could also be detected as a periodic Doppler shift and the enhancement of emission in the blue wing of the emission line (e.g., Banerjee et al. 2009; Kitagawa et al. 2010; Verwichte et al. 2010). Many authors studied the speed of propagating disturbances detected simultaneously at different EUV wavelengths, corresponding to different temperatures (e.g., King et al. 2003; Kiddie et al. 2012; Uritsky et al. 2013). The speed of the EUV disturbances situated at nonsunspot regions was not found to show a clear dependence on the temperature, whereas those disturbances propagating above the sunspots show a clear temperature dependence. In particular, Uritsky et al. (2013) estimated the speed of a propagating wave in warm fan-like structures, and found that the speed obeys a square-root temperature dependence predicted for slow magnetoacoustic waves, i.e., the phase speed of the disturbance increases with the plasma temperature. Analysis of the relationship between relative density and temperature perturbations in those waves allowed to estimate the value of the adiabatic index  $\gamma$  (Van Doorsselaere et al. 2011).

The period of the coronal slowly propagating EUV intensity perturbations is likely to be determined by the conditions at the footpoints of the coronal waveguiding structures. Chae & Goode (2015) showed that, in response to impulsive disturbances, the gravitationally stratified atmosphere came to oscillate along the field with a period determined by the

acoustic cut-off frequency. There is a possibility of leakage of these oscillations along the magnetic fan structures to the corona as was demonstrated numerically by Botha et al. (2011), and observationally by Sych et al. (2009, 2015).

Propagating slow magnetoacoustic waves in coronal plasma structures are usually observed to damp rapidly with height. Theoretical modeling has addressed several mechanisms potentially responsible for the wave amplitude evolution, such as thermal conduction, viscosity, gravitational stratification, magnetic flux tube divergence, field geometry, and nonlinear cascade (e.g., Nakariakov et al. 2000b; Ofman et al. 2000; Tsiklauri & Nakariakov 2001; De Moortel & Hood 2003; Ofman 2005; Selwa et al. 2005; Owen et al. 2009). In particular, it has been found numerically that the damping lengths vary with the periods (Gupta 2014; Mandal et al. 2016). The vast majority of these studies has been performed in the approximation of the infinite magnetic field, when the model describes the plasma flows strictly along the magnetic field. In other words, the waves have been considered as plane acoustic waves with the wave fronts perpendicular to the field. This one-dimensional approach is well justified in the case when the effect of the magnetic field on the plasma motions dominates, in other words, when the ratio of the gas and magnetic pressures, known as the plasma parameter  $\beta$ , is very small. However, it is known that in the finite  $\beta$  case, the effects of the wave front obliqueness, which are intrinsic for the waves guided by field-aligned plasma nonuniformities, become important. In particular, in this regime, the speed of the slow magnetoacoustic waves propagating apparently along the field approaches the subsonic and sub-Alfvénic tube (cusp) speed (e.g., Roberts & Webb 1978), the cut-off frequency (Roberts 2006; Zhugzhda & Sych 2014; Afanasyev & Nakariakov 2015a) becomes dependent on the magnetic field, the effectiveness of the nonlinear cascade decreases (Afanasyev & Nakariakov 2015b), and the geometrical dispersion is introduced (Zhugzhda & Goossens 2001). If the parallel, along the field, wavelength of the perturbations is much longer than the transverse size of the waveguiding plasma nonuniformity, the obliqueness effects could be accounted for by the thin flux tube approximation (e.g., Roberts & Webb 1979; Zhugzhda 1996) that reduces the three-dimensional consideration to a one-dimensional one too. However, it is still not clear how so rapidly damped coronal slow waves could reach the heights of about one solar radius above the surface, for example, detected by Ofman et al. (1997).

Another important physical effect that is intrinsic for the corona is the apparent thermal equilibrium of the waveguiding plasma structures. Indeed, as coronal field-aligned plasma nonuniformities, such as loops and plumes, have lifetimes much longer than the radiative cooling and thermal conductive times, there must be a process that compensates the losses of the internal energy, the enigmatic coronal heating process (e.g., Parnell & De Moortel 2012, for a recent review). Thermal equilibrium should be taken into account in the consideration of MHD wave dynamics together with the mechanical equilibrium. A compressive wave can modify differently the different equilibrium quantities responsible for the internal energy losses and gains, e.g., the density, temperature, magnetic field, causing a local thermal equilibrium misbalance (i.e., the “cooling/heating misbalance”) that, in turn, affects the wave dynamics (e.g., Nakariakov et al. 2000a). The effect of the cooling/heating misbalance has been intensively studied in

the context of the cool prominence formation and oscillation (e.g., Arregui et al. 2012, for a comprehensive review). The main attention was paid to the enhanced damping of the oscillations caused by the nonadiabatic effects and induced plasma condensation. For hotter plasma structures, it was recently shown that the cooling/heating misbalance could significantly modify the damping and nonlinear evolution of standing slow magnetoacoustic waves in coronal loops (Kumar et al. 2016). In the latter work, the effects of the finite plasma- $\beta$  were neglected.

The aim of this paper is to study the effect of the local cooling/heating misbalance on long-wavelength slow magnetoacoustic waves guided by a field-aligned plasma nonuniformity, in terms of the thin flux tube approximation. The mathematical formalism is similar to that adopted by Afanasyev & Nakariakov (2015b), with additional terms in the dispersion relation and the evolutionary equation, which account for the effect of the cooling/heating misbalance. The paper is organized as follows. In Section 2, we present and discuss the governing equations. In Section 3, we derive the wave equation for weakly nonlinear slow waves in the presence of finite thermal conduction, viscosity, and plasma- $\beta$ , and allowing for the local thermal equilibrium misbalance. In Section 4, we obtain dispersion relations, and determine the threshold of the thermal over-stability. In Section 5, we derive and analyze the Burgers–Malthus equation that describes the slow wave evolution in the presence of weakly nonlinear, dissipative, and cooling/heating misbalance effects. Our findings are summarized and discussed in Section 6.

## 2. Governing Equations and Equilibrium

Dynamics of long-wavelength slow magnetoacoustic waves in a straight untwisted and nonrotating field-aligned plasma nonuniformity is described by the first-order thin flux tube approximation derived by Roberts & Webb (1978) and Zhugzhda (1996). The governing equations comprise the energy, momentum, transverse total pressure balance, induction, mass continuity, and state equations,

$$\frac{dp}{dt} - \frac{\gamma p}{\rho} \frac{d\rho}{dt} = (\gamma - 1) \left[ Q(\rho, T, B) + \kappa \frac{\partial^2 T}{\partial z^2} \right], \quad (1)$$

$$\rho \left( \frac{\partial u}{\partial t} + u \frac{\partial u}{\partial z} \right) + \frac{\partial p}{\partial z} = \frac{2}{3} \eta \frac{\partial v}{\partial z} + \frac{4}{3} \eta \frac{\partial^2 u}{\partial z^2}, \quad (2)$$

$$p + \frac{B^2}{8\pi} = p_T^{\text{ext}}, \quad (3)$$

$$\frac{\partial B}{\partial t} + u \frac{\partial B}{\partial z} + 2Bv = 0, \quad (4)$$

$$\frac{\partial \rho}{\partial t} + 2\rho v + \frac{\partial}{\partial z}(\rho u) = 0, \quad (5)$$

$$p = \frac{k_B}{m} \rho T, \quad (6)$$

where  $\rho$  is the plasma density,  $p$  is the plasma pressure,  $T$  is the temperature,  $u$  is the speed of bulk flow along the tube,  $v$  is the radial derivative of the radial component of the plasma velocity, and  $B$  is the longitudinal component of magnetic field strength. All of these parameters are measured at the axis of the flux tube; and  $p_T^{\text{ext}}$  is the total external pressure. The coefficient  $\gamma$  is the adiabatic index,  $k_B$  is the Boltzmann

constant, and  $m$  is the mean particle mass, i.e., about a half of the proton mass. The coefficients  $\eta$  and  $\kappa$  describe the viscosity and field-aligned thermal conduction, respectively.

The function  $Q(\rho, T, B)$  is the cooling/heating function that accounts for the optically thin radiative cooling and coronal heating. The radiative cooling can be modeled by the expression  $\rho^2 T(T)$ . The function  $T$  depends on the temperature of the plasma. This dependence, especially its fine structure, based on the detailed knowledge of the atomic physics effects associated with the presence of minor species, is not known exactly. Different authors give rather different dependences in the temperature range from a few to several millions of K (e.g., Schure et al. 2009; Soler et al. 2012). In almost all cases, the derivative of  $T$  with respect to the temperature is highly nonmonotonic in the coronal temperature range (e.g., Somov et al. 2007). Also, as the specific heating mechanism of the coronal plasma remains unknown, we assume that the heating function depends, in general, on the thermodynamical parameters, i.e., the temperature  $T$  and density  $\rho$ , and possibly the magnetic field  $B$  too (e.g., Hood 1992). Because of those uncertainties in both radiative cooling and heating functions, we treat the derivatives of the function  $Q(\rho, T, B)$  with respect to its arguments in the thermal equilibrium as free parameters.

The set of Equations (1)–(6) is similar to the equations used in Afanasyev & Nakariakov (2015b), but in addition accounts for the effects of field-aligned thermal conduction and cooling/heating misbalance. The set of Equations (1)–(6) does not include the rotation of the flux tube and the magnetic field twist. These two quantities are assumed to be zero in the equilibrium. Their perturbations constitute a torsional wave that is linearly decoupled from the slow magnetoacoustic wave (e.g., Vasheghani Farahani et al. 2011), and hence is not considered in our analysis. Also, we neglect the effects associated with the dispersion connected with the finite ratio of the flux tube diameter and wavelength, i.e., the geometrical dispersion, discussed in Zhugzhda & Goossens (2001). The effects of the field-aligned nonuniformity of the plasma, in particular, the appearance of the tube cut-off frequency (e.g., Roberts 2006; Zhugzhda & Sych 2014; Afanasyev & Nakariakov 2015a), are also neglected.

### 3. Dynamics of Small Perturbations

Consider perturbations of a mechanical equilibrium that are characterized by constant quantities  $p_0, \rho_0, B_0, T_0$ , and  $p_T^{\text{ext}}$ , without steady flows. In addition, the thermal equilibrium  $Q(\rho_0, T_0, B_0) = 0$  is fulfilled, i.e., the heating compensates the radiative losses in the equilibrium. The parallel thermal conduction does not contribute to the equilibrium, as the equilibrium temperature is constant. We assume that the effects of quadratic nonlinearity, dissipation and local radiation/heating misbalance are weak and of the same order of magnitude with each other. Let the perturbations of the equilibrium physical quantities be small,

$$\begin{aligned} p &= p_0 + p_1, \quad \rho = \rho_0 + \rho_1, \quad T = T_0 + T_1, \\ B &= B_0 + B_1, \quad v = v_1, \quad u = u_1, \end{aligned} \quad (7)$$

where the subscript 1 denotes small but finite perturbations. In the following, we omit this subscript for the variables  $u$  and  $v$ .

Following the procedure described in Afanasyev & Nakariakov (2015b) and Kumar et al. (2016), we substitute expansion (7) in Equations (1)–(6) and, taking into account quadratically nonlinear

terms everywhere except the terms on the right-hand sides of Equations (1) and (2), where we keep linear terms only, we obtain

$$\begin{aligned} \frac{\partial p_1}{\partial t} - C_S^2 \frac{\partial \rho_1}{\partial t} &= -u \frac{\partial p_1}{\partial z} + C_S^2 u \frac{\partial \rho_1}{\partial z} + \gamma \frac{\rho_1}{\rho_0} \frac{\partial p_1}{\partial t} \\ &+ (\gamma - 1) \left( a_\rho \rho_1 + a_T T_1 + a_B B_1 + \kappa \frac{\partial^2 T_1}{\partial z^2} \right) \\ &+ \frac{[\gamma p_1 - C_S^2 (\gamma + 1) \rho_1] \partial \rho_1}{\rho_0 \partial t}, \end{aligned} \quad (8)$$

$$\begin{aligned} \rho_0 \frac{\partial u}{\partial t} + \frac{\partial p_1}{\partial z} &= -\rho_0 u \frac{\partial u}{\partial z} - \rho_1 \frac{\partial u}{\partial t} \\ &+ \frac{2}{3} \eta \frac{\partial v}{\partial z} + \frac{4}{3} \eta \frac{\partial^2 u}{\partial z^2}, \end{aligned} \quad (9)$$

$$p_1 + \frac{B_0 B_1}{4\pi} = -\frac{B_1^2}{8\pi}, \quad (10)$$

$$\frac{\partial B_1}{\partial t} + 2B_0 v = -u \frac{\partial B_1}{\partial z} - 2v B_1, \quad (11)$$

$$\frac{\partial \rho_1}{\partial t} + 2\rho_0 v + \rho_0 \frac{\partial u}{\partial z} = -2\rho_1 v - \frac{\partial}{\partial z}(\rho_1 u), \quad (12)$$

$$p_1 - \frac{k_B}{m}(\rho_0 T_1 + T_0 \rho_1) = \frac{k_B}{m} T_1 \rho_1, \quad (13)$$

where  $C_S^2 = \gamma p_0 / \rho_0$  is the sound speed. We use the Taylor expansion of the cooling/heating function  $Q$  near the equilibrium, with  $a_\rho = \partial Q / \partial \rho$ ,  $a_T = \partial Q / \partial T$ , and  $a_B = \partial Q / \partial B$  taken at  $\rho_0, T_0$ , and  $B_0$ , respectively. As mentioned above, in our study, we consider the values of  $a_\rho, a_T$ , and  $a_B$  to be unknown, and hence treat them as free parameters. We use the standard expressions for the estimation of the field-aligned thermal conductivity,  $\kappa \approx 10^{-11} T^{5/2} \text{ W m}^{-1} \text{ K}^{-1}$  and the dynamic viscosity,  $\eta \approx 10^{-17} T^{5/2} \text{ kg m}^{-1} \text{ s}^{-1}$  (e.g., De Moortel & Hood 2003), and hence neglect the possible enhancement of the transport coefficients by micro-turbulence. Both the nonlinear and nonadiabatic terms that are assumed to be small are gathered on the right-hand sides of the equations. With the use of the expression  $C_S^2 = \gamma k_B T_0 / m$ , the ideal gas law given by Equation (13) can be written as

$$p_1 - \frac{C_S^2}{\gamma} \left( \frac{\rho_0}{T_0} T_1 + \rho_1 \right) = \frac{C_S^2}{\gamma T_0} T_1 \rho_1. \quad (14)$$

The total pressure  $p_T^{\text{ext}}$  in the external medium was assumed to be constant, and consequently the effect of the slow magnetoacoustic waves on the external medium was neglected. This assumption is justified if the phase speed of the wave is lower than the characteristic speeds in the external medium (see the discussion in Roberts & Webb 1979; Zhugzhda 1996). However, the perturbation of the external medium must be accounted for in the consideration of the fast magnetoacoustic wave (e.g., Vasheghani Farahani et al. 2014).

Eliminating all the variables in Equations (8)–(13) in favor of  $u$  being a natural variable of a slow magnetoacoustic wave,

we obtain the wave equation

$$\begin{aligned} \frac{\partial}{\partial t} \left[ \frac{\partial^2 u}{\partial t^2} - C_T^2 \frac{\partial^2 u}{\partial z^2} \right] &= \frac{\rho_0 C_T}{C_S^2} \frac{\partial}{\partial t} \left[ \frac{\mathcal{N}}{(C_S^2 + V_A^2)} \right] \\ &+ \frac{(\gamma - 1)^2 C_T^2 \kappa T_0}{C_S^2 \rho_0} \frac{\partial^4 u}{\partial z^4} - \frac{(\gamma - 1)^2 \kappa T_0}{(C_S^2 + V_A^2) \rho_0} \frac{\partial^4 u}{\partial t^2 \partial z^2} \\ &- \frac{\eta C_T^2}{3 \rho_0 V_A^2} \frac{\partial^4 u}{\partial t^2 \partial z^2} - \frac{4 \eta C_T}{3 \rho_0} \frac{\partial^4 u}{\partial t \partial z^3} \\ &- \frac{(\gamma - 1)}{(C_S^2 + V_A^2) \rho_0} \mathcal{A} \frac{\partial^2 u}{\partial t^2} + \frac{(\gamma - 1) C_T^2}{C_S^2 \rho_0} \mathcal{A} \frac{\partial^2 u}{\partial z^2}, \end{aligned} \quad (15)$$

where  $V_A = B_0 / (4\pi\rho_0)^{1/2}$  is the Alfvén speed,  $C_T = C_S V_A / (C_S^2 + V_A^2)^{1/2}$  is the tube (also called “cusp”) speed, and  $\mathcal{N}$  is the quadratically nonlinear term,

$$\begin{aligned} \mathcal{N} &= \frac{C_S^4 V_A^2}{C_T^2 \rho_0} \frac{\partial}{\partial z} \left( u \frac{\partial u}{\partial z} \right) + \frac{C_S^2 V_A^2}{C_T \rho_0} \frac{\partial}{\partial z} \left( u \frac{\partial u}{\partial t} \right) \\ &+ \frac{(\gamma - 1) C_S^2}{\rho_0} \frac{\partial}{\partial t} \left( u \frac{\partial u}{\partial t} \right) - \frac{C_S^4}{V_A^2 \rho_0} \frac{\partial}{\partial t} \left( u \frac{\partial u}{\partial t} \right) \\ &- \frac{B_0}{4\pi} \frac{\partial}{\partial t} \left[ \frac{B_0 C_S^4}{C_T V_A^2 \rho_0^2} \left( u \frac{\partial u}{\partial z} \right) + \frac{4\pi C_S^4}{B_0 V_A^2 \rho_0} \left( u \frac{\partial u}{\partial t} \right) \right] \\ &+ V_A^2 \frac{\partial}{\partial t} \left[ \frac{4\pi C_S^2}{B_0^2} \left( u \frac{\partial u}{\partial t} \right) - \frac{C_S^2}{C_T \rho_0} \left( u \frac{\partial u}{\partial z} \right) \right], \end{aligned} \quad (16)$$

and the derivatives of the cooling/heating functions at the equilibrium are combined in the parameter

$$\mathcal{A} = a_\rho \rho_0 + (\gamma - 1) a_T T_0 - \frac{a_B B_0 C_S^2}{V_A^2}. \quad (17)$$

In the derivation, we neglected terms that contain products of the coefficients  $\kappa$  and  $\eta$  with each other and also with  $a_\rho$ ,  $a_T$ , and  $a_B$ , taking that the associated effects are small in the considered case of weak dissipation and cooling/heating misbalance.

In addition, we obtain the linear relations of variables  $p_1$ ,  $\rho_1$ ,  $B_1$ ,  $T_1$ , and  $v$  with  $u$ ,

$$\begin{aligned} p_1 &\approx \rho_0 C_T u, \quad \rho_1 \approx \rho_0 \frac{C_T}{C_S^2} u, \quad B_1 \approx -\frac{B_0 C_T}{V_A^2} u, \\ v &\approx \frac{C_T}{2V_A^2} \frac{\partial u}{\partial t}, \quad T_1 \approx \frac{(\gamma - 1) T_0 C_T}{C_S^2} u, \end{aligned} \quad (18)$$

which are obtained from the left-hand side of the set of Equations (8)–(13), neglecting the nonlinear and nonadiabatic terms.

Equation (15) is a self-consistent partial differential equation for a single scalar variable  $u$ , and can be used for modeling the dynamics of a weakly nonlinear, weakly nonadiabatic slow magnetoacoustic wave guided by a magnetic flux tube, accounting for the effects of weak nonlinearity, weak dissipation, and weak misbalance of the radiative losses and unspecified heating. These equations contain only one dependent variable  $u(z, t)$ . In the linear, adiabatic limit the right-hand side of Equation (15) is zero, and the equation reduces to the standard wave equation describing two waves of

an arbitrarily smooth shape propagating in the opposite directions along the field at the speed  $C_T$ .

It is evident that in the small plasma- $\beta$  limit,  $C_S/V_A \rightarrow 0$ , the speed  $C_T$  tends to the sound speed  $C_S$ , and the perturbations of the magnetic field and the perpendicular flow speed in the slow magnetoacoustic wave vanish. Thus, the wave becomes purely longitudinal, with the plasma flows directed strictly along the equilibrium magnetic field. Therefore, in the  $\beta \rightarrow 0$  limit one can use the infinite field approximation, describing the slow magnetoacoustic waves guided by the magnetic flux tube as plane acoustic waves. In this limit, Equation (15) reduces to

$$\begin{aligned} \frac{\partial}{\partial t} \left[ \frac{\partial^2 u}{\partial t^2} - C_S^2 \frac{\partial^2 u}{\partial z^2} \right] &= \frac{\rho_0}{C_S} \frac{\partial}{\partial t} \left[ \frac{\mathcal{N}_{(C_S \ll V_A)}}{V_A^2} \right] \\ &+ \frac{(\gamma - 1)^2 \kappa T_0}{\rho_0} \frac{\partial^4 u}{\partial z^4} - \frac{4\eta C_S}{3\rho_0} \frac{\partial^4 u}{\partial t \partial z^3} \\ &+ \frac{(\gamma - 1)}{\rho_0} \mathcal{A}_{(C_S \ll V_A)} \frac{\partial^2 u}{\partial z^2}, \end{aligned} \quad (19)$$

where

$$\begin{aligned} \mathcal{N}_{(C_S \ll V_A)} &= \frac{C_S^2 V_A^2}{\rho_0} \frac{\partial}{\partial z} \left( u \frac{\partial u}{\partial z} \right) + \frac{C_S V_A^2}{\rho_0} \frac{\partial}{\partial z} \left( u \frac{\partial u}{\partial t} \right) \\ &+ \frac{(\gamma - 1) C_S^2}{\rho_0} \frac{\partial}{\partial t} \left( u \frac{\partial u}{\partial t} \right) - \frac{\partial}{\partial t} \left[ \frac{C_S^3}{\rho_0} \left( u \frac{\partial u}{\partial z} \right) \right] \\ &+ \frac{\partial}{\partial t} \left[ \frac{C_S^2}{\rho_0} \left( u \frac{\partial u}{\partial t} \right) - \frac{C_S V_A^2}{\rho_0} \left( u \frac{\partial u}{\partial z} \right) \right]. \end{aligned} \quad (20)$$

#### 4. Linear Dispersion Relation

Neglecting nonlinear terms, we assume the harmonic dependence of perturbed quantities on time  $t$  and the field-aligned coordinate  $z$ ,  $\propto \exp(-i\omega t + ikz)$ , where  $\omega$  is the frequency and  $k$  is the parallel wavenumber, and obtain from Equation (15) the dispersion relation

$$\begin{aligned} \omega^2 - C_T^2 k^2 &\approx -i \left\{ \frac{(\gamma - 1)^2 C_T^2 \kappa T_0}{\rho_0 \omega C_S^2} k^4 \right. \\ &- \frac{(\gamma - 1)^2 \kappa T_0}{\rho_0 (C_S^2 + V_A^2)} \omega k^2 - \frac{\eta C_T^2}{3\rho_0 V_A^2} \omega k^2 + \frac{4\eta C_T}{3\rho_0} k^3 \\ &\left. + \frac{(\gamma - 1)(\omega^2 - V_A^2 k^2)}{\omega \rho_0 (C_S^2 + V_A^2)} \mathcal{A} \right\}. \end{aligned} \quad (21)$$

This equation has been derived under the assumption that the nonadiabatic effect caused by the finite thermal conduction, viscosity, and misbalance of radiation and heating is small. Thus, the terms on the right-hand side are much smaller than on the left-hand side. Considering the waves that propagate in the positive direction of  $z$ , and taking that the wavenumber  $k$  is real, we obtain  $\omega \approx C_T k$  and  $\omega_R \gg \omega_I$ , where  $\omega_R$  and  $\omega_I$  are the real and imaginary parts of the frequency, respectively.



Thus, dispersion relation (21) can be simplified to

$$\omega \approx C_T k - i \left[ \frac{(\gamma - 1)^2 \kappa T_0 C_T^2}{2\rho_0 C_S^4} + \frac{\eta}{6\rho_0} \left( 3 + \frac{V_A^2}{C_S^2 + V_A^2} \right) \right] k^2 + \frac{i(\gamma - 1) C_T^2}{2\rho_0 C_S^4} \mathcal{A}. \quad (22)$$

Hence, the real and imaginary parts of omega are

$$\omega_R \approx C_T k, \quad (23)$$

$$\omega_I \approx \mathcal{P} k^2 + \mathcal{R}, \quad (24)$$

respectively, where

$$\mathcal{P} = - \left[ \frac{(\gamma - 1)^2 \kappa T_0 C_T^2}{2\rho_0 C_S^4} + \frac{\eta}{6\rho_0} \left( 3 + \frac{V_A^2}{C_S^2 + V_A^2} \right) \right],$$

$$\mathcal{R} = \frac{(\gamma - 1) C_T^2}{2\rho_0 C_S^4} \mathcal{A}. \quad (25)$$

The imaginary part of the frequency, given by Equation (24) consists of two terms. The first term,  $\mathcal{P}$ , that accounts for the effects of the thermal conductivity  $\kappa$  and viscosity  $\eta$ , is always negative, and hence always contributes to the damping of the slow waves. The damping time is inversely proportional to  $k^2$ , i.e., the waves of shorter wavelengths decay more rapidly than those of longer ones. This is consistent with the previous findings (see, e.g., Nakariakov et al. 2000b; De Moortel & Hood 2003; Mandal et al. 2016).

The second term,  $\mathcal{R}$ , can be either positive or negative, depending on the local dependences of the cooling/heating function  $Q(\rho, T, B)$  on its arguments at the equilibrium. When  $\mathcal{R} < 0$  this term contributes to damping. However, the damping caused by this term is independent of  $k$ . In the case  $\mathcal{R} > 0$ , this term suppresses damping, and can even lead to the increase in the wave amplitude, the phenomenon known as thermal over-stability (e.g., see Nakariakov et al. 2000a; Kumar et al. 2016, for this effect on magnetoacoustic waves). The critical value of  $\mathcal{R}$  that separates the damping and over-stable regimes is

$$\mathcal{R}^{\text{crit}} = \left[ \frac{(\gamma - 1)^2 \kappa T_0 C_T^2}{2\rho_0 C_S^4} + \frac{\eta}{6\rho_0} \left( 3 + \frac{V_A^2}{C_S^2 + V_A^2} \right) \right] k^2. \quad (26)$$

For  $\mathcal{R} > \mathcal{R}^{\text{crit}}$ , the plasma becomes thermally over-stable, and a slow magnetoacoustic perturbation grows in time. The value of  $\mathcal{R}^{\text{crit}}$  reduces with the increase in the oscillation wavelength,  $2\pi/k$ .

## 5. Weakly Nonlinear Wave Evolution

Following the procedure described in detail in Afanasyev & Nakariakov (2015b; see, also, Nakariakov et al. 2000b), we adopt the single-wave approximation, and use Equation (15) to derive the evolutionary equation for the weakly nonlinear

perturbations,

$$\frac{\partial u}{\partial Z} = -\alpha_{\text{NL}} u \frac{\partial u}{\partial \xi} + \alpha_{\text{D}} \frac{\partial^2 u}{\partial \xi^2} + \alpha_{\text{M}} u,$$

$$\alpha_{\text{NL}} = \frac{C_T}{2(C_S^2 + V_A^2)} \left[ 3 + (\gamma + 1) \frac{V_A^2}{C_S^2} \right],$$

$$\alpha_{\text{D}} = \frac{(\gamma - 1)^2 \kappa T_0 C_T}{2\rho_0 C_S^4} + \frac{\eta}{6\rho_0 C_T} \left( 3 + \frac{V_A^2}{C_S^2 + V_A^2} \right),$$

$$\alpha_{\text{M}} = \frac{(\gamma - 1) C_T}{2\rho_0 C_S^4} \left[ a_\rho \rho_0 + (\gamma - 1) a_T T_0 - \frac{a_B B_0 C_S^2}{V_A^2} \right], \quad (27)$$

where we introduced the new independent variables  $\xi = z - C_T t$  and  $Z = \epsilon z$  in the frame of reference moving at the tube speed  $C_T$ ,  $\epsilon$  is a small parameter characterizing the weak rate of the wave evolution caused by the right-hand-side terms in Equation (15). In the limit  $\kappa = 0$ , and  $\mathcal{R} = 0$ , Equation (27) reduces to the Burgers equation for slow waves, derived by Afanasyev & Nakariakov (2015b). In the case when the effects of the local radiation/heating misbalance are small but finite, Equation (27) is a generalized Burgers equation with an additional linear term (the ‘‘Malthus’’ term) that accounts for the effect of nonzero derivatives of the radiative cooling/heating function. This equation can be called the Burgers–Malthus equation, or a version of the Burgers–Fisher equation with a linear reaction term. The coefficients  $\alpha_{\text{NL}}$  and  $\alpha_{\text{D}}$  are always positive, while  $\alpha_{\text{M}}$  can be either positive or negative, depending upon the specific form of the cooling/heating misbalance. In the case of a negligibly small initial amplitude and dissipation,  $\alpha_{\text{NL}} = 0$  and  $\alpha_{\text{D}} = 0$ , Equation (27) reduces to the Malthus equation.

In the limit  $C_S \ll V_A$ , the coefficients in Equation (27) reduce to

$$\alpha_{\text{NL}} = \frac{(\gamma + 1)}{2C_S},$$

$$\alpha_{\text{D}} = \frac{(\gamma - 1)^2 \kappa T_0}{2\rho_0 C_S^3} + \frac{2\eta}{3\rho_0 C_S},$$

$$\alpha_{\text{M}} = \frac{(\gamma - 1)}{2\rho_0 C_S^3} [a_\rho \rho_0 + (\gamma - 1) a_T T_0], \quad (28)$$

and the governing equation corresponds to the case of plane acoustic waves.

### 5.1. Analytical Estimations

It is possible to estimate the characteristic distances of the evolutionary processes caused separately by the specific mechanisms. If the effects of nonlinearity and radiative cooling/heating misbalance are neglected,  $\alpha_{\text{NL}} = 0$  and  $\alpha_{\text{M}} = 0$ , respectively, and the initial perturbation is assumed to be harmonic,  $u(\xi, Z = 0) \propto \sin(k\xi)$ , where  $k$  is the wavenumber, one obtains that  $u \propto \exp(-Z/Z_D)$ , where  $Z_D = (\alpha_{\text{D}} k^2)^{-1}$  is the damping length. For a fixed oscillation period,  $P$ , using  $k = 2\pi(C_T P)^{-1}$ , the damping length becomes

$$Z_D = \frac{C_T^2 P^2}{4\pi^2 \alpha_{\text{D}}}. \quad (29)$$

Considering the values of  $Z_D$  to be caused separately by thermal conduction and viscosity, described by the first and second terms, respectively, on the right-hand side of the expression for  $\alpha_D$ , one can compare the effects of these dissipative mechanisms on the slow wave. In particular, for the broad range of the typical parameters of nonflaring active regions, the temperature  $7 \times 10^5 - 2 \times 10^6$  K, and the mass density  $10^{-14} - 10^{-10}$  kg m $^{-3}$ , the ratio of the values of  $Z_D$  caused only by thermal conduction and only by viscosity is from 2.5 to 14.4. Thus, in the corona, the effect of thermal conduction on the slow wave damping is stronger than of viscosity, which is consistent with the findings of De Moortel & Hood (2003). In the low- $\beta$  limit, the dependence of the ratio of the damping length to the wavelength can be estimated as

$$\frac{Z_D}{C_T P} \approx \frac{\rho_0 P}{T_0^{3/2}}. \quad (30)$$

For  $\alpha_M \neq 0$ , and still neglecting nonlinear effects, the damping length becomes  $Z_D = (\alpha_D k^2 - \alpha_M)^{-1}$ , or

$$Z_D = \frac{C_T^2 P^2}{4\pi^2 \alpha_D - C_T^2 P^2 \alpha_M}. \quad (31)$$

This expression is consistent with dispersion relations (23) and (24). For  $\alpha_M < 0$  ( $\mathcal{R} < 0$ ), the cooling/heating misbalance decreases the damping length; while for  $\alpha_M > 0$  it increases it. In the particular case  $\alpha_M = \alpha_M^{\text{crit}} = 4\pi^2 \alpha_D / C_T^2 P^2$  that corresponds to  $\mathcal{R} = \mathcal{R}^{\text{crit}}$ , the oscillation becomes decayless,  $Z_D = \infty$ . For  $\alpha_M > \alpha_M^{\text{crit}}$ , an over-stability takes place ( $Z_D < 0$ ), see Equation (26). In the limit  $\alpha_D \ll \alpha_M$ ,  $Z_D \approx -\alpha_M^{-1}$ , and the over-stability occurs for any  $\alpha_M > 0$ .

Neglecting the dissipative effects,  $\alpha_D = 0$ , but accounting for nonlinear effects, Equation (27) has the implicit solution

$$u - F \left\{ \xi - \frac{\alpha_{\text{NL}}}{\alpha_M} [1 - \exp(-\alpha_M Z)] u \right\} \exp(\alpha_M Z) = 0, \quad (32)$$

where the function  $F(\xi)$  is the profile of the wave at the initial time,  $u(\xi, Z = 0) = F(\xi)$  (e.g., Nakariakov et al. 2000a). This equation describes the nonlinear steepening of the initial perturbation. The distance at which the wave breaks, i.e., the shock is formed, is given by the expression

$$Z_B = \frac{1}{\alpha_M} \log \left( 1 - \frac{\alpha_M}{\alpha_{\text{NL}}} f' \right), \quad (33)$$

where  $f'$  is the value of the derivative of the function  $f$  at the inflection point, with  $f$  being the inverse function of the initial shape of the wave,  $\xi = f(u)$ , i.e.,  $f$  is the function inverse to  $F$ . In particular, for  $u(\xi, Z = 0) = A \sin(k\xi)$ ,  $f' = (Ak)^{-1}$ . As  $\alpha_{\text{NL}} > 0$ , the shock forms at the slope with the negative derivate,  $\partial F / \partial \xi < 0$ . We would like to stress that in the expressions in this section the amplitude  $A$  is dimensional, having the units of the speed. For an initially harmonic wave, the expression for the breaking distance becomes

$$Z_B = \frac{1}{\alpha_M} \log \left( 1 + \frac{\alpha_M}{\alpha_{\text{NL}} Ak} \right) = \frac{1}{\alpha_M} \log \left( 1 + \frac{\alpha_M C_T P}{2\pi \alpha_{\text{NL}} A} \right). \quad (34)$$

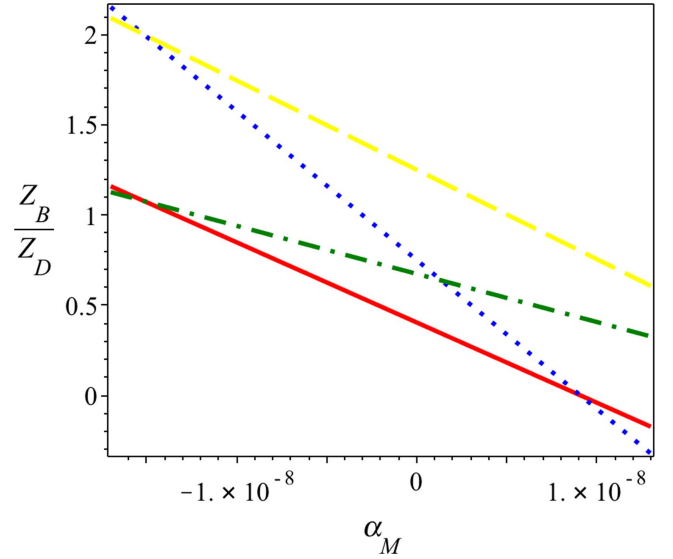


**Figure 1.** Dependence of the ratio of the breaking and damping distances on the parameter of the cooling/heating misbalance in a plasma with the temperature 700,000 K, mass density  $10^{-12}$  kg m $^{-3}$ , and magnetic field 10 G. The red (solid) curve corresponds to a tube wave of the period of 300 s and with the initial amplitude of  $1.3 \times 10^4$  m s $^{-1}$ ; the blue (dotted) to the period of 180 s and amplitude of  $1.3 \times 10^4$  m s $^{-1}$ ; the yellow (dashed) to the period of 180 s and amplitude of  $7 \times 10^3$  m s $^{-1}$ ; and the green (dotted-dashed) to the period of 300 s and amplitude of  $7 \times 10^3$  m s $^{-1}$ .

For  $\alpha_M \rightarrow 0$ , the breaking distance is  $Z_B = -f' / \alpha_{\text{NL}}$ . For an initially harmonic wave, the breaking distance is

$$Z_B = \frac{1}{\alpha_{\text{NL}} Ak} = \frac{C_T P}{2\pi \alpha_{\text{NL}} A} \quad (35)$$

(see, e.g., Afanasyev & Nakariakov 2015b, for a discussion).

The ratio  $Z_B / Z_D$  determines the mutual importance of the effects of nonlinear steepening and damping. Figure 1 shows the dependence of this ratio on the value of  $\alpha_M$ . We can see that the cooling/heating misbalance affects the relative importance of nonlinear and dissipative effects rather significantly, and thus should be taken into account. In a general case when  $Z_B$  and  $|Z_D|$  are of the same order of magnitude, estimating expressions (31) and (35) should be used with caution, because of the mutual influence of the effects of nonlinear steepening, dissipation and either enhanced or reduced damping or over-stability due to the cooling/heating misbalance.

## 5.2. Numerical Solutions

To illustrate the possible scenarios of the wave evolution in the case when all three considered physical mechanisms, the nonlinearity, dissipation, and cooling/heating misbalance, operate simultaneously, we solve Equation (27) numerically with the use of the *pdsolve* function of *Maple 2016.1*.

Figure 2 shows the effect of the cooling/heating misbalance on the slow wave evolution in a typical coronal active region loop. The left panel corresponds to the case without the misbalance. The wave experiences slight steepening caused by the nonlinear cascade, and decay because of the dissipation caused by thermal conduction and viscosity. This behavior is consistent with the models developed in Nakariakov et al. (2000b), Ofman et al. (2000), and Afanasyev & Nakariakov (2015b). The middle panel shows the over-stable regime caused by a positive  $\alpha_M$ . In this case, the cooling/heating misbalance amplifies the wave more

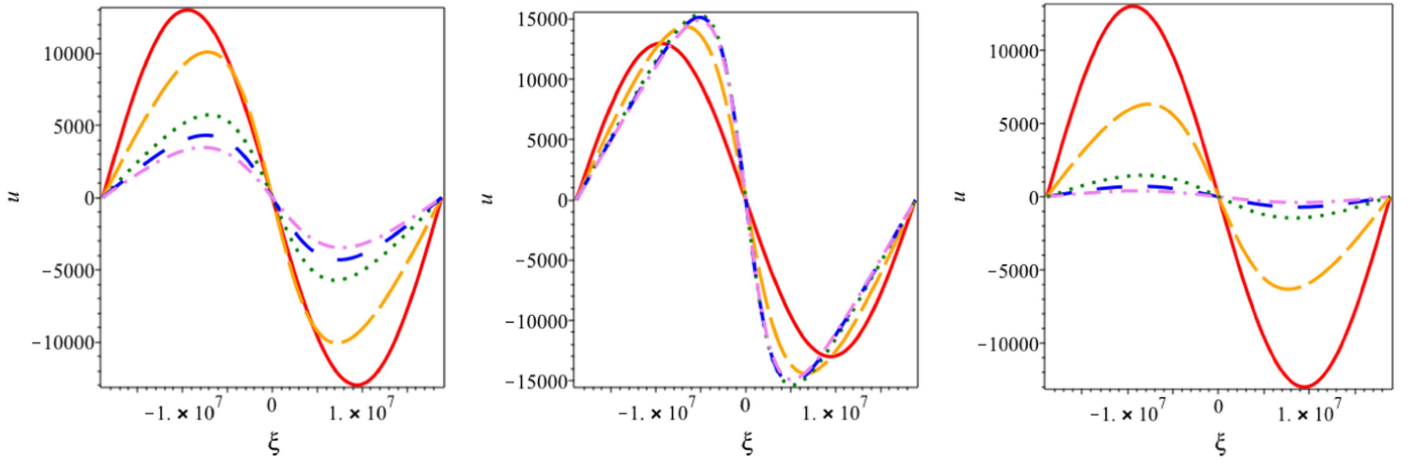


**Figure 2.** Evolution of the shape of an initially harmonic slow magnetoacoustic wave of the period of 300 s and with the initial amplitude of  $1.3 \times 10^4 \text{ m s}^{-1}$ , guided by a plasma cylinder with the plasma of the temperature 700,000 K, mass density  $10^{-12} \text{ kg m}^{-3}$ , and magnetic field 10 G, which corresponds to the sound speed of  $1.27 \times 10^5 \text{ m s}^{-1}$ , Alfvén speed of  $8.92 \times 10^5 \text{ m s}^{-1}$ , and tube speed of  $1.26 \times 10^5 \text{ m s}^{-1}$ . Left panel: the effect of the misbalance of radiative cooling and heating is neglected. The red (solid) curve shows the initial shape of the wave. The orange (long-dash) curve at the distance 27.5 Mm from the wave origin; the green (dotted) at 82.5 Mm; the blue (dash) at 110 Mm; and the violet (dashed-dotted) at 132 Mm. The distance along the cylinder  $\xi$  is given in meters, and the wave amplitude  $u$  in meters per second. Middle panel: the same, but for  $\alpha_M = 1.3 \times 10^{-8} \text{ m}^{-1}$ . Right panel: the same, but for  $\alpha_M = -1.7 \times 10^{-8} \text{ m}^{-1}$ .

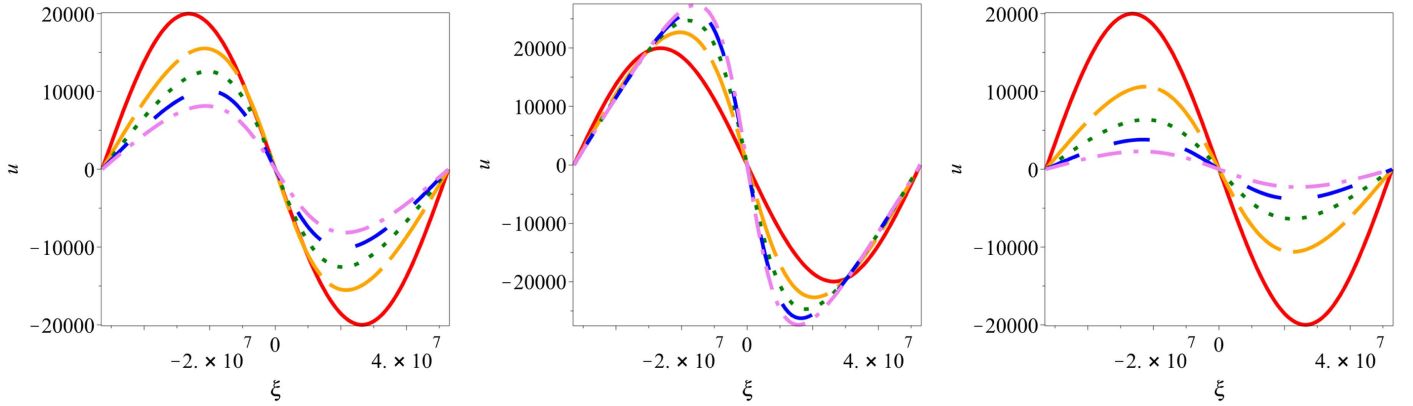


**Figure 3.** Evolution of the shape of an initially harmonic slow magnetoacoustic wave of the period of 600 s and with the initial amplitude of  $2 \times 10^4 \text{ m s}^{-1}$ , guided by a plasma cylinder with the plasma of the temperature  $1.4 \times 10^6 \text{ K}$ , mass density  $10^{-12} \text{ kg m}^{-3}$ , and magnetic field 1 G, which corresponds to the sound speed of  $1.79 \times 10^5 \text{ m s}^{-1}$ , Alfvén speed of  $8.92 \times 10^5 \text{ m s}^{-1}$ , and tube speed of  $1.76 \times 10^5 \text{ m s}^{-1}$ . Left panel: the effect of the misbalance of radiative cooling and heating is neglected. The red (solid) curve shows the initial shape of the wave. The orange (long-dash) curve at the distance 54 Mm from the wave origin; the green (dotted) at 98 Mm; the blue (dash) at 141 Mm; and the violet (dashed-dotted) at 184 Mm. The distance along the cylinder  $\xi$  is given in meters, and the wave amplitude  $u$  in meters per second. Middle panel: the same, but for  $\alpha_M = 7 \times 10^{-9} \text{ m}^{-1}$ . Right panel: the same, but for  $\alpha_M = -7 \times 10^{-9} \text{ m}^{-1}$ .

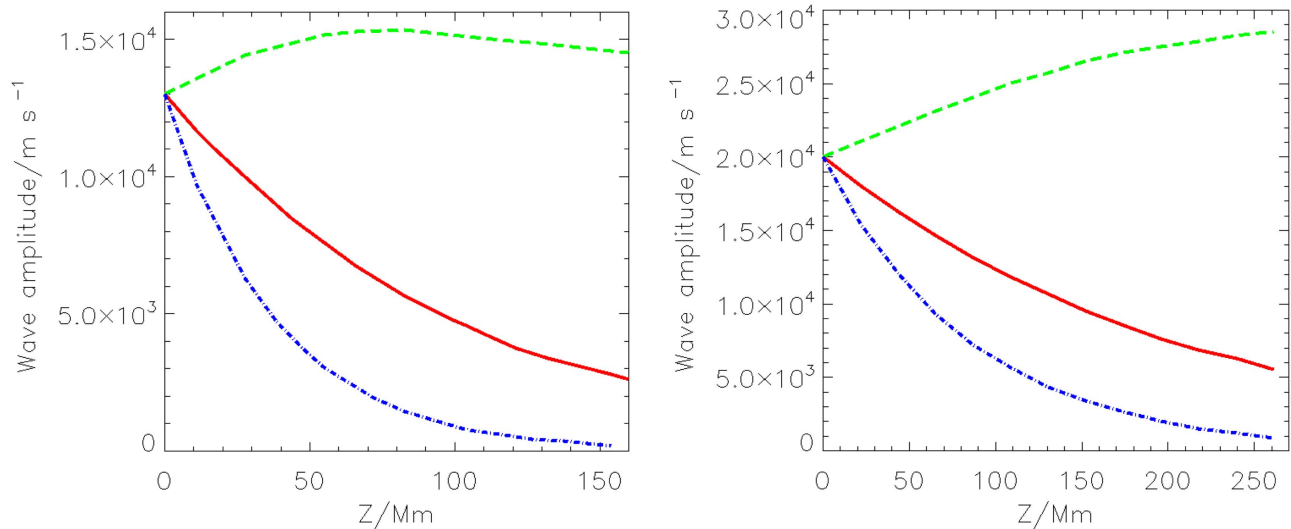
effectively than the dissipation causes the wave decay, and the wave amplitude increases—the effect of the thermal over-stability of slow magnetoacoustic waves. Because of the suppressed decay, the nonlinear cascade effectively steepens the wave shape, forming a shock at the negative slope. When the wave becomes sufficiently steep, the dissipation that enhances with the wave steepening because of its dependence on the wavenumber squared, stops the further increase in the wave amplitude. The right panel shows the case of a negative  $\alpha_M$ . In this case, the cooling/heating misbalance contributes to the wave damping. In this case, the wave amplitude decreases with the travel distance much more rapidly than it is caused by thermal conduction and viscosity (see the left panel). Figure 3 shows a similar behavior, but for the conditions typical for a polar plume. The effect of the cooling/heating misbalance on a slow wave is similar to the case of a coronal loop, discussed above.

Figure 4 shows the variation of the wave amplitude with the distance from the origin for the same conditions as in Figures 2 and 3. It is evident that the cooling/heating misbalance may either increase the wave damping or counteract the dissipation.

The gradual decrease in the amplification seen in the green (dashed) curves that correspond to the over-stable case, is attributed to the increase in the dissipation because of the nonlinear cascade—the effect of nonlinear dissipation. In the left panel, because of this effect the amplitude reaches the maximum and then begins decreasing when the wave becomes sufficiently steep. In the right panel, this regime is not evident, and the over-stable wave seems to reach some saturation when the amplitude and the saw-tooth shape remain the same during the wave propagation. The latter case corresponds to a so-called stationary wave regime (e.g., Chin et al. 2010).

## 6. Discussion and Conclusions

Assuming the effects of nonlinearity, dissipation connected with finite thermal conduction and viscosity, and misbalance of the radiative losses and unspecified heating to be weak, we derived a self-consistent wave equation describing the propagation of long-wavelength slow magnetoacoustic waves guided by a cylindrical field-aligned nonuniformity of a finite- $\beta$



**Figure 4.** Evolution of the slow wave amplitude along a plasma cylinder. The red (solid) curves show the case  $\alpha_M = 0$ , green (dashed) curves  $\alpha_M = 7 \times 10^{-9} \text{ m}^{-1}$ , and blue (dotted-dashed) curves  $\alpha_M = -7 \times 10^{-9} \text{ m}^{-1}$ . Left panel: the parameters of the plasma and wave are the same as in the middle panel of Figure 2. Right panel: the parameters of the plasma and wave are the same as in the right panel of Figure 2.

plasma. This equation contains only one dependent variable, and hence provides us with a convenient ground for the study of the wave evolution by asymptotic techniques, addressing the effects of nonlinearity, dissipation, and activity of the waveguiding medium. The effect of the activity of the medium occurs when a wave gets amplified during its propagation. In the considered case, the activity is caused by the cooling/heating misbalance.

Using the single-wave approximation, we reduced the wave equation to a Burgers–Malthus evolutionary equation that generalizes the Burgers equation derived in Afanasyev & Nakariakov (2015b) by accounting for the effects of the finite thermal conduction and cooling/heating misbalance. It is established that the slow wave behavior is very sensitive to the particular features of the dependences of the radiative cooling/heating function on the physical quantities perturbed by the wave, i.e., the plasma density and temperature, and the magnetic field. Depending upon the specific combination of the derivatives of the cooling/heating function with respect to the density, temperature, and the magnetic field, taken at the equilibrium, and dissipation, slow magnetoacoustic waves may experience enhanced or reduced damping, or amplification. In the latter case, there is no violation of the energy conservation, as the considered system is nonconservative, because of the energy supply by the heating, i.e., the plasma acts as an active medium for the magnetoacoustic waves. The strength of this effect depends upon the steepness of the radiative cooling/heating function, which is still unknown. For example, we could expect the dependence of the heating function upon the magnetic field to be quite steep in the case of cyclotron resonance mechanisms.

If the wave amplitude is sufficiently high, e.g., exceeds several percent of the equilibrium value, or the wave amplification by thermal over-stability is stronger than the damping by dissipation, the wave experiences nonlinear steepening because of the nonlinear cascade. It may either lead to the nonlinear dissipation that is much stronger for the same value of the transport coefficients than the dissipation in the linear regime (see, e.g., Afanasyev & Nakariakov 2015b), or to the occurrence of a stationary regime similar to that

described in Chin et al. (2010), in which the wave has a sawtooth shape but the amplitude does not decay. This phenomenon could be understood in terms of the wave spectrum evolution. The terms on the right-hand side of Equation (27) affect the wave spectrum differently. The first, nonlinear term causes the nonlinear cascade via the continuous doubling of the wavenumber. In other words, this term is responsible for the energy transfer to larger wave numbers. The second, dissipative term causes the conversion of the wave energy into the internal energy of the medium, which is most effective for larger wave numbers. The enhanced, nonlinear dissipation occurs when these two effects operate together: the nonlinearity transfers the wave energy from longer wavelengths where the dissipation is ineffective, to the shorter wavelengths where this energy is effectively dissipated. In the presence of the third term that describes the cooling/heating misbalance, the wave is either amplified or decayed, depending on the sign of the coefficient  $\alpha_M$ . It occurs with the same effectiveness for all wave numbers. In the over-stable regime, there could be a balance between the energy supply, transfer to larger wave numbers, and dissipation, which causes the occurrence of stationary, i.e., non-evolving, propagating waves.

In several important limiting cases, namely when either the dissipation, or cooling/heating misbalance, or nonlinearity are negligible, we obtained simple estimations for the characteristic distances of the wave evolution. The wave damping and breaking lengths are found to be determined by the wave parameters (period, amplitude), and properties of the medium (density, temperature, magnetic field, and the cooling/heating function). These estimations allow one to assess the relative importance of different physical effects in the slow wave evolution in specific cases.

The results obtained provide us with a starting point for the possible seismological estimation of the coronal heating function and therefore identifying its mechanism. However, this perspective requires the precise knowledge of the radiative cooling function. In addition, in realistic coronal plasma structures for the observed periods of the slow waves, i.e., several minutes, it may be important to account for stratification. In particular, the stratification causes the increase in the



amplitude of the slow wave propagating upwards (see, e.g., Nakariakov et al. 2000b; Ofman et al. 2000). Hence, the variation of the wave amplitude caused by the cooling/heating misbalance, is additive to the amplification due to the stratification. In the over-stable regime the cooling/heating misbalance acts together with the amplification by stratification. Also, recent observational findings indicate a possible departure of the thermal conductivity and dynamical viscosity coefficients from the standard estimations (Wang et al. 2015). It would be of interest to check whether this discrepancy could be attributed to the effect of the cooling/heating misbalance. In addition, the results obtained could possibly explain the occurrence of periodic compressive disturbances at the coronagraph heights (e.g., Ofman et al. 1997). A possible scenario could be a variation of the coefficient  $\alpha_M$  with height, which leads to the amplification of the slow waves propagating upward in a certain range of heights. A dedicated study of this effect would be of interest too.



The main outcome of this work is the demonstration that the cooling/heating misbalance can affect slow magnetoacoustic waves rather significantly, and may be responsible for certain discrepancies between the previously obtained theoretical results and observations. In particular, this effect can cause additional, wavelength-independent damping of the waves, or, otherwise, counteract the damping by finite thermal conduction and viscosity. We would like to point out that the wave damping is determined by the dependences of the cooling/heating misbalance function on the plasma parameters, and not by the actual cooling or heating time of the plasma structure. Another interesting application of the obtained results is connected with the excitation of slow magnetoacoustic (for example, the “longitudinal”) oscillations in filaments. For example, the simultaneous occurrence of transverse and longitudinal oscillations by a shock wave, observed by Shen et al. (2014). The slow magnetoacoustic oscillation in a filament could be excited by a sudden change of the cooling/heating misbalance in the filament plasma, caused by the interaction with the shock. More specifically, the excitation could take place when the sudden modification of the cooling/heating misbalance changes the sign of  $\alpha_M$ . Thus, a further modeling of this effect seems to be of interest for both hot and cool coronal plasma structures. In particular, this study could contribute to revealing the mechanisms for the excitation of large amplitude oscillations in prominences (Arregui et al. 2012). Also, the Burgers–Malthus evolutionary equation derived here provides one with a starting point for the analytical model of standing slow magnetoacoustic waves in hot plasma loops, following the formalism developed in Ruderman (2013) and Kumar et al. (2016), based on the use of Equation (27).

We would also point out that this study demonstrated that in the finite  $\beta$  case the slow wave in a field-aligned plasma waveguide perturbs the absolute value of the magnetic field in the waveguide. The magnetic field perturbation is in anti-phase with the perturbation of the plasma density (see Equation (18)). It may have an interesting effect on the thermal radio emission from coronal plasma structures, modulating it via the wave-induced variations of the electron plasma frequency and electron gyrofrequency.

This work is supported by the BK21 plus program through the National Research Foundation funded by the Ministry of

Education of Korea (V.M.N., S.K., Y.J.M.); the European Research Council under the *SeismoSun* Research Project No. 321141 (V.M.N.); and the Russian Science Foundation under grants 17-72-10076 (A.N.A.: analytical derivations and analysis of the wave evolution).

## ORCID iDs

V. M. Nakariakov  <https://orcid.org/0000-0001-6423-8286>  
Y.-J. Moon  <https://orcid.org/0000-0001-6216-6944>

## References

- Abedini, A. 2016, *Ap&SS*, 361, 133  
 Afanasyev, A. N., & Nakariakov, V. M. 2015a, *A&A*, 582, A57  
 Afanasyev, A. N., & Nakariakov, V. M. 2015b, *A&A*, 573, A32  
 Arregui, I., Oliver, R., & Ballester, J. L. 2012, *LRSP*, 9, 2  
 Banerjee, D., Teriaca, L., Gupta, G. R., et al. 2009, *A&A*, 499, L29  
 Berghmans, D., & Clette, F. 1999, *SoPh*, 186, 207  
 Botha, G. J. J., Arber, T. D., Nakariakov, V. M., & Zhugzhda, Y. D. 2011, *ApJ*, 728, 84  
 Chae, J., & Goode, P. R. 2015, *ApJ*, 808, 118  
 Chin, R., Verwichte, E., Rowlands, G., & Nakariakov, V. M. 2010, *PhPI*, 17, 032107  
 DeForest, C. E., & Gurman, J. B. 1998, *ApJL*, 501, L217  
 De Moortel, I. 2009, *SSRv*, 149, 65  
 De Moortel, I., & Browning, P. 2015, *RSPTA*, 373, 20140269  
 De Moortel, I., & Hood, A. W. 2003, *A&A*, 408, 755  
 De Moortel, I., Ireland, J., & Walsh, R. W. 2000, *A&A*, 355, L23  
 Gupta, G. R. 2014, *A&A*, 568, A96  
 Hood, A. W. 1992, *PPCF*, 34, 411  
 Jess, D. B., Morton, R. J., Verth, G., et al. 2015, *SSRv*, 190, 103  
 Kiddie, G., De Moortel, I., Del Zanna, G., McIntosh, S. W., & Whittaker, I. 2012, *SoPh*, 279, 427  
 King, D. B., Nakariakov, V. M., Deluca, E. E., Golub, L., & McClements, K. G. 2003, *A&A*, 404, L1  
 Kitagawa, N., Yokoyama, T., Imada, S., & Hara, H. 2010, *ApJ*, 721, 744  
 Krishna Prasad, S., Banerjee, D., & Van Doorselaere, T. 2014, *ApJ*, 789, 118  
 Krishna Prasad, S., Banerjee, D., Van Doorselaere, T., & Singh, J. 2012, *A&A*, 546, A50  
 Kumar, S., Nakariakov, V. M., & Moon, Y.-J. 2016, *ApJ*, 824, 8  
 Mandal, S., Magyar, N., Yuan, D., Van Doorselaere, T., & Banerjee, D. 2016, *ApJ*, 820, 13  
 Marsh, M. S., Walsh, R. W., & Plunkett, S. 2009, *ApJ*, 697, 1674  
 Nakariakov, V. M. 2006, *RSPTA*, 364, 473  
 Nakariakov, V. M., Mendoza-Briceño, C. A., & Ibáñez, S. M. H. 2000a, *ApJ*, 528, 767  
 Nakariakov, V. M., Pilipenko, V., Heilig, B., et al. 2016, *SSRv*, 200, 75  
 Nakariakov, V. M., Verwichte, E., Berghmans, D., & Robbrecht, E. 2000b, *A&A*, 362, 1151  
 Ofman, L. 2005, *SSRv*, 120, 67  
 Ofman, L., Nakariakov, V. M., & Sehgal, N. 2000, *ApJ*, 533, 1071  
 Ofman, L., Romoli, M., Poletto, G., Noci, G., & Kohl, J. L. 1997, *ApJL*, 491, L111  
 Owen, N. R., De Moortel, I., & Hood, A. W. 2009, *A&A*, 494, 339  
 Parnell, C. E., & De Moortel, I. 2012, *RSPTA*, 370, 3217  
 Roberts, B. 2006, *RSPTA*, 364, 447  
 Roberts, B., & Webb, A. R. 1978, *SoPh*, 56, 5  
 Roberts, B., & Webb, A. R. 1979, *SoPh*, 64, 77  
 Ruderman, M. S. 2013, *A&A*, 553, A23  
 Sakao, T., Kano, R., Narukage, N., et al. 2007, *Sci*, 318, 1585  
 Schure, K. M., Kosenko, D., Kaastra, J. S., Keppens, R., & Vink, J. 2009, *A&A*, 508, 751  
 Selwa, M., Murawski, K., & Solanki, S. K. 2005, *A&A*, 436, 701  
 Shen, Y., Liu, Y. D., Chen, P. F., & Ichimoto, K. 2014, *ApJ*, 795, 130  
 Soler, R., Ballester, J. L., & Parenti, S. 2012, *A&A*, 540, A7  
 Somov, B. V., Dzhililov, N. S., & Staude, J. 2007, *AstL*, 33, 309  
 Su, J. T. 2014, *ApJ*, 793, 117  
 Sych, R., Karlický, M., Altyntsev, A., Dudík, J., & Kashapova, L. 2015, *A&A*, 577, A43  
 Sych, R., Nakariakov, V. M., Karlický, M., & Anfinogentov, S. 2009, *A&A*, 505, 791  
 Tsiklauri, D., & Nakariakov, V. M. 2001, *A&A*, 379, 1106

- Uritsky, V. M., Davila, J. M., Viall, N. M., & Ofman, L. 2013, [ApJ](#), **778**, 26
- Van Doorselaere, T., Wardle, N., Del Zanna, G., et al. 2011, [ApJL](#), **727**, L32
- Vasheghani Farahani, S., Hornsey, C., Van Doorselaere, T., & Goossens, M. 2014, [ApJ](#), **781**, 92
- Vasheghani Farahani, S., Nakariakov, V. M., van Doorselaere, T., & Verwichte, E. 2011, [A&A](#), **526**, A80
- Verwichte, E., Marsh, M., Foullon, C., et al. 2010, [ApJL](#), **724**, L194
- Wang, T., Ofman, L., Sun, X., Provornikova, E., & Davila, J. M. 2015, [ApJL](#), **811**, L13
- Yuan, D., & Nakariakov, V. M. 2012, [A&A](#), **543**, A9
- Yuan, D., Nakariakov, V. M., Chorley, N., & Foullon, C. 2011, [A&A](#), **533**, A116
- Zhugzhda, Y. D. 1996, [PhPI](#), **3**, 10
- Zhugzhda, Y. D., & Goossens, M. 2001, [A&A](#), **377**, 330
- Zhugzhda, Y. D., & Sych, R. A. 2014, [AstL](#), **40**, 576